~~Plasma fusion show~~ Meeting of the APS plasma physics division
of APS.
New York, NY,USA, October 12 - 16, 1981.
CEA - CONF 6066.

FR 8201113

INTERACTION FAISCEAUX DE PROTONS-CIBLE A DES DENSITES DE PUISSANCE FAIBLES ET ELEVEES

B. DUBORGEL - J.M. DUFOUR - Ph. GOUARD

RESUME

L'interaction de faisceaux d'ions légers avec des cibles variées est calculée à partir d'un modèle de dépôt d'énergie des ions couplé à un code hydrodynamique, prenant en compte l'évolution du plasma pendant le chauffage de la cible.

Les calculs sont faits dans 2 cas :

- aux faibles densités de puissance possibles sur une machine de laboratoire comme SIDONIX

- aux densités de puissance élevées demandées pour la fusion.

Dans le cas des faibles densités de puissance, les conditions requises pour des expériences d'implosion de cibles susceptibles de mettre en évidence la production de neutrons thermonucléaires sont discutées. La simulation des processus de dépôt aux densités de puissance élevées montre que les caractéristiques du dépôt d'énergie sont fortement modifiées pendant le chauffage de la cible.

Proton beams-target interaction at low and high power densities - B.DUBORGEL, J.M.DUFOUR, Ph.GOUARD - C.E.A., Centre d'Etudes de Limeil, BP N°27, 94190 VILLENEUVE SAINT GEORGES, FRANCE

Interaction of light ions beams with various targets is calculated from an ion energy deposition model coupled with an hydrodynamic code, taking account of the plasma evolution during the target heating.

The calculations are made in two cases : at low power densities available on a laboratory machine as SIDONIX, at high power densities required for pellet fusion. In the case of low power densities the requirements of a neutron target implosion experiment are discussed. The simulation of deposition processes at high power densities shows that the energy deposition characteristics are strongly modified during the target heating.

INTRODUCTION

INTRODUCTION

Our study of light ion - target interaction concerns two domains of power densities.

1)- Low power densities available on a laboratory machine as SIDONIX

. SIDONIX machine (in Valduc) is converted in light ion generator.

at present time : light ion beam production has been obtained with pinch reflex diode (200 kA 1 MeV deutons) /1 / /2 /

next step : beam focus to $J \gtrsim 200\ kA/cm^2$

Energy deposition calculations described in this paper correspond to this hypothesis $J \sim 200\ kA/cm^2$.

. Objectives of Sidonix light ion programme : hydrodynamic experiments.

thin foils heating

ablative and exploding pusher regimes study

two foils acceleration

conditions of a neutron monobeam implosion experiment in a conical target.

2)- High power densities required to pellet fusion

Energy deposition calculations were extended to high power densities $\sim 100 - 200\ TW/cm^2$ required to pellet fusion :

to evaluate range shortening in ionized matter

to conceive target and ablator structures.

For example, energy deposition calculations are given for 4 MeV proton beam incident on gold target ($E \sim 1$ MJ, $P_s \sim 200\ TW/cm^2$).

1 - ION ENERGY DEPOSITION MODEL. DEPION CODE /3 /

Physical approximations of the model are those used by different authors, especially Mehlhorn /4 / .

1-1 - Stopping power of cold material

$$\frac{dE}{dS}\left(\varepsilon = \frac{E}{A_1}\ \text{MeV/amu}\right)_T = \frac{dE}{dS}_{e^-} + \frac{dE}{dS}_n$$

1-1-1 - Electronic stopping power

. $\varepsilon \leqslant \varepsilon_1 = 0.025\ Z_1^{2/3}$ MeV/amu

$$\frac{dE}{dS}_{e^-\ LSS} = \chi \cdot \frac{dE}{dS}_{LSS}$$

$\chi\ (Z_1, A_1, Z_2, A_2)$: factor by which the formula of Lindhard-Scharff-Schiott's model must be multiplied to give the best fit to the low energy experimental data.

. $\varepsilon \geqslant \varepsilon_2 = 0{,}4$ MeV/amu $= \overline{\varepsilon}_2\ (T = 0,\ \rho = \rho_o)$

$$\frac{dE}{dS}_{e^-\ Bethe} = \frac{4\pi\ Z_1^{*2} e^4}{m_e c^2\ \beta^2}\ \frac{N_e}{\rho}\left[\ln \frac{2m_e c^2\ \beta^2\ \gamma^2}{\overline{I}} - \beta^2 - \frac{C}{Z_2} - \frac{\delta}{2}\right] = \frac{4\pi\ Z_1^{*2} e^4}{m_e c^2 \beta^2}\frac{N_e}{\rho},$$

Bethe's theory shell corrections from the formalism adapted by Andersen-Ziegler.

. $\varepsilon_1 \leqslant \varepsilon \leqslant \varepsilon_2$ Joining by polynomial form

$$\ln \frac{dE}{dS}_{e^-} = \sum_{n=0}^{3} C_n\ (\ln \varepsilon)^n$$

1-1-2 - Nuclear stopping power

$\frac{dE}{dS}_n$ at low specific energies : Steward-Wallace's formalism adjusted with Lindhard's model.

.../...

1-2 - Stopping power of heated and expanded material

$$\left.\frac{dE}{dS}\right)_T = \left.\frac{dE}{dS}\right)_{\text{bound } e^-} + \left.\frac{dE}{dS}\right)_{\text{free } e^- \text{ plasma}} + \left.\frac{dE}{dS}\right)_{\text{ion plasma}}$$

Target heating can vary

from 10 - 50 eV (laboratory machine)

to several hundreds eV (power installation).

Target plasma state characterized by the degree of material ionization $\overline{Z_2}$ (T , ρ).

Calculation of $\overline{Z_2}$ at thermodynamic equilibrium, and following LATTE in the Thomas-Fermi model of a spherical mean atom.

. Bound electron stopping power ($Z_2 - \overline{Z_2}$ (T, ρ))

$\left.\frac{dE}{dS}\right)_{\text{cold}}$ modified by Mehlhorn with $\overline{I}$ (T, ρ)

$\overline{\varepsilon_2}$(T, ρ) is calculated so that $\Delta\left[\overline{\varepsilon_2}(T, \rho)\right] = \Delta\left[\overline{\varepsilon_2}(T = 0,\ \rho = \rho_o)\right]$

and $\overline{\varepsilon_2}(T, \rho) > \overline{\varepsilon_2}$ $(T = 0, \rho = \rho_o)$ = 0,4 MeV /amu.

. plasma electron and plasma ion stopping power

calculated from Jackson's formalism with a maxwellian distribution of particle plasma velocities.

The general expression is similar to the Bethe's formula and can be written as

$$\left.\frac{dE}{dS}\right)_f = \frac{4\pi\, Z_1^{*2}\, Z_f^2\, e^4}{m_f\, v^2}\ \frac{n_f}{\rho}\ \ln \Lambda_f \ .\ G\,(y_f)$$

f indice relative to the particle plasma.

$\ln \Lambda_f$ takes account of binary collisions and excitation of collective plasma oscillations.

.../...

1-3 - Pathlength

. mean total pathlength $\overline{S_T}$ of a projectile ion slowing down from ε_o energy to $\varepsilon < \varepsilon_o$ energy

$$\overline{S_T}\,(\varepsilon, \varepsilon_o) = A_1 \int_{\varepsilon}^{\varepsilon_o} \frac{d\,\varepsilon}{\frac{dE}{dS}(\varepsilon)_T} \quad g/cm^2$$

. For high Z_2 targets and light ion beams of low energy, the mean projected range is shorter (some %) than the mean pathlength because the small angle multiple scattering.

In cold material, the mean projected range $\overline{S_p}$ is calculated by Schiott or Biersack's formalism

$$\overline{S_p} = \int \langle \cos \varphi \rangle \; dS = \int_o^{E_o} e^{-2\tau(E_o,E)} \; \frac{dE}{\frac{dE}{dS}(E)_T}$$

$$\tau = -\frac{A_2}{A_1} \int_{E_o}^{E} \frac{\frac{dE}{dS}n}{\frac{dE}{dS}T} \frac{dE}{E}$$

Example : 1 MeV proton beam incident on cold gold target. Fig.1

1-4 - Multi-shell Targets

. multi-atomic composite material for compound targets

Bragg additivity rule relating the stopping power of a compound to that of its constituents.

Example : 1 MeV proton beam incident on cold glass target. Fig. 2

. multi-shell target with constituents of arbitrary composition, density, temperature.

Example : 10 MeV proton beam incident on a heated and expanded gold target. Fig.3

.../...

DEPION CALCULATIONS

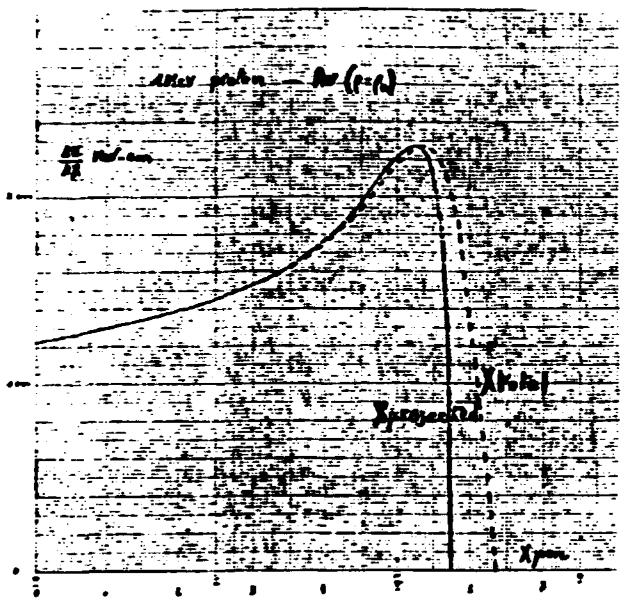

Fig.1 - 1 MeV proton range in cold gold target

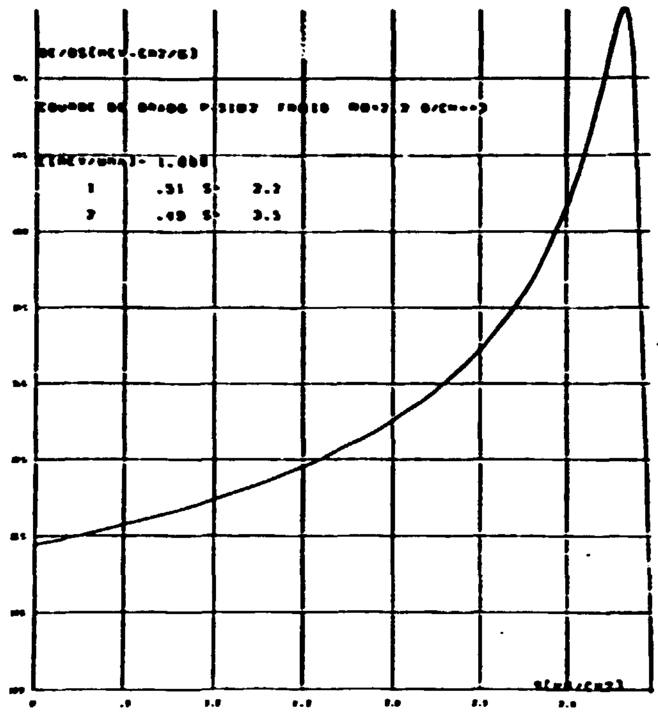

Fig.2 - 1 MeV proton range in cold glass target

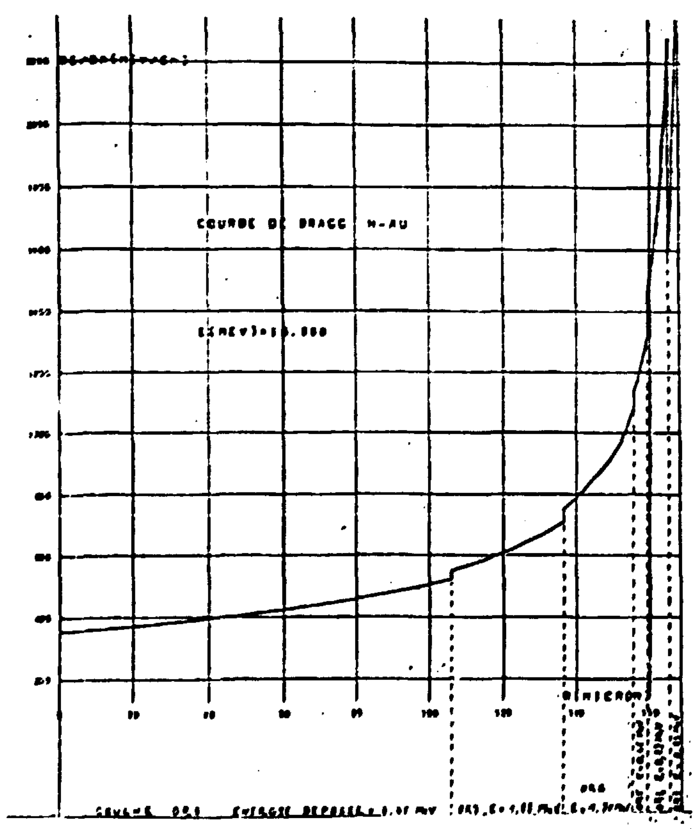

Fig. 3 - 10 MeV proton range in multishell target (heated and expanded gold target)

2 - SIMULATION OF TARGET HEATING

The coupling of DEPION with and hydrodynamic code provides, at each time of the pulse, the characteristics of depositionand the corresponding state of plasma.

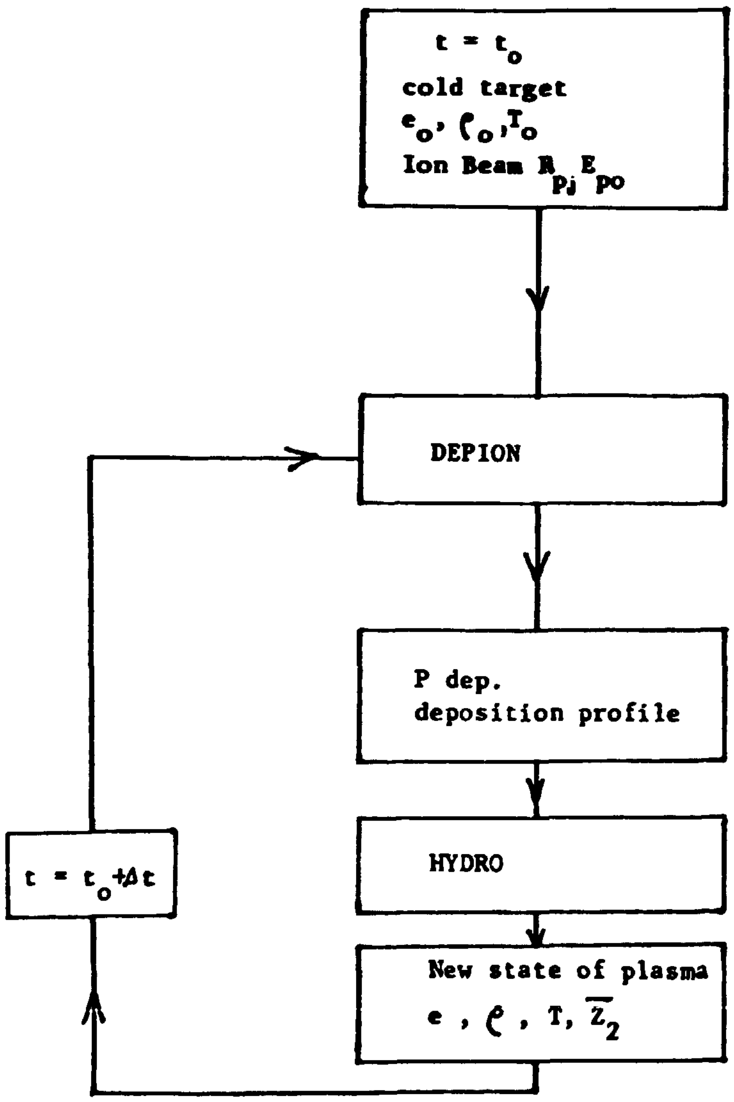

Simulations results are directly comparable with experimental diagnostics : XRD and target temperature measurements, foil hydrodynamic (e, v...) etc...

.../...

3 - LIGHT ION-TARGET INTERACTION AT LOW POWER DENSITIES - SIDONIX EXPERIMEN PREVISIONS

Beam data hypothesis $\begin{cases} 1 \text{ MeV protons} \quad J \sim 200 \text{ kA/cm}^2 \quad \Delta t \sim 30 \text{ ns} \\ \Rightarrow \overline{P} \sim 0{,}2 \text{ TW/cm}^2 \quad E \sim 6 \text{ KJ/cm}^2 \end{cases}$

3-1 - Low Z target : CH2

3-1-1 - Energy deposition evolution during the target heating

DEPION's evaluations

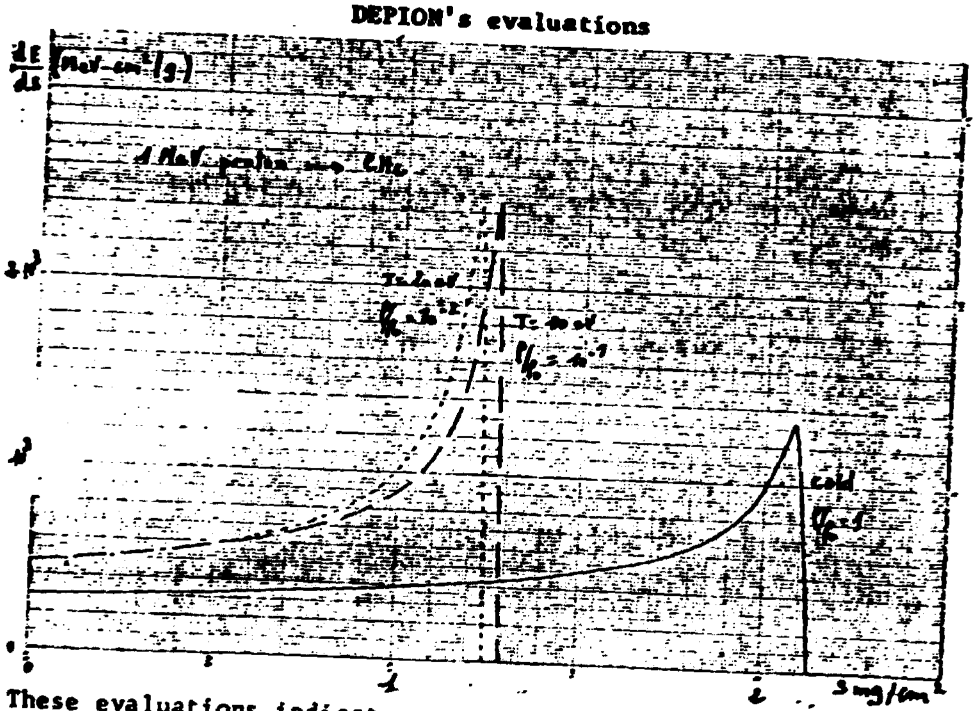

Fig.4

These evaluations indicate a strong reduction of the proton range; but the calculations are not very precise at low densities and temperatures.

3-1-2 - Hydrodynamic experiments previsions

- Foils acceleration : ablative or exploding pusher regimes study
- Exploding pusher implosion in a conical target (monobeam)

target $\phi \sim 3$ mm

only a low part of the beam to have a good irradiation uniformity.

ρ_o DT $\sim 3.10^{-5}$ g/cm^3

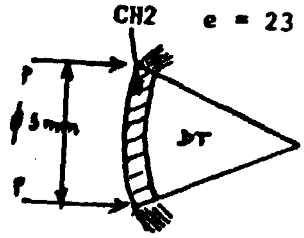

Energy deposition in CH2

T_{max} ablator $\sim$ 15-20 eV

.../...

Calculated implosion characteristics

- v_{max} compression $\sim$ 5.10^{6} cm/s in CH2, $\sim$ 10^{7} cm/s in DT
- $T_{max\ DT} \sim$ 500 to 800 eV
- $\int \rho\ dr \sim 5.10^{-4}$
- Number of neutrons $\sim 4.10^{6}$

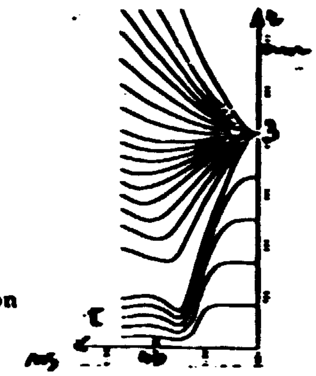

Fig.5

Implosion diagram

3-2 - High Z target : Au

3-2-1 - Energy deposition evolution during the target heating

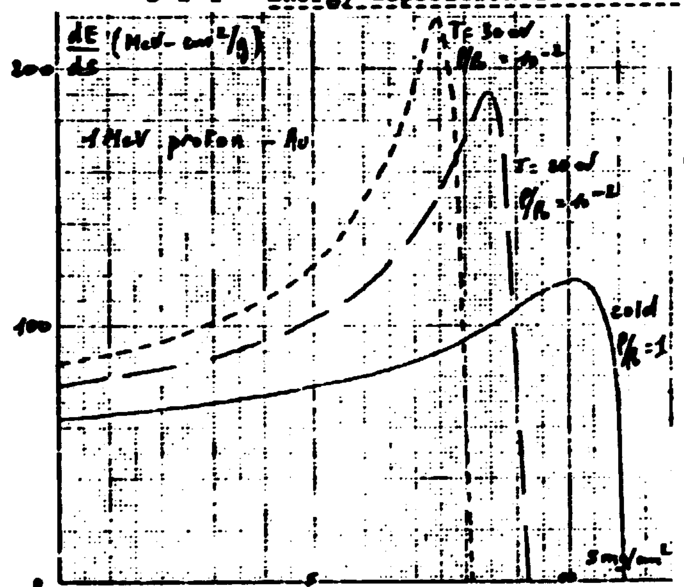

DEPION's evaluations

These evaluations show a significative shortening of the proton range in this domain; but calculations are not very precise at low densities and temperatures.

Fig.6

3-2-2 - Hydrodynamic experiments previsions

- Foils acceleration : ablative or exploding pusher regimes study
- Implosions in a conical target (monobeam)

.../....

- monoshell target

T_{max} ablator ∽ 25 eV

calculated implosion characteristics ϕ=3mm

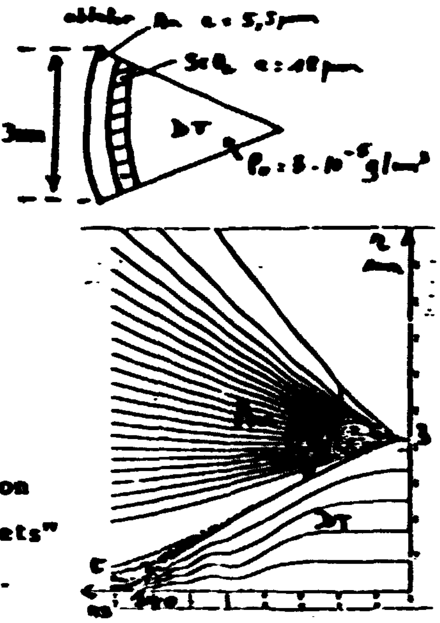

v_{max} pusher ∽ 3.10^6 cm/s

T_{max} DT ∽ 300 to 500 eV

$\int \rho\, dr$ ∽ $3,6.10^{-3}$

Number of neutrons ∽ 10^7

Long, slow and quasi isentropic implosion

But : high r/Δr target as "russian targets"

⟹ hydrodynamic instability problem.

Fig.7 - Implosion diagram

- double shell target

⟹ velocity multiplication

calculated implosion characteristics ϕ=3 mm

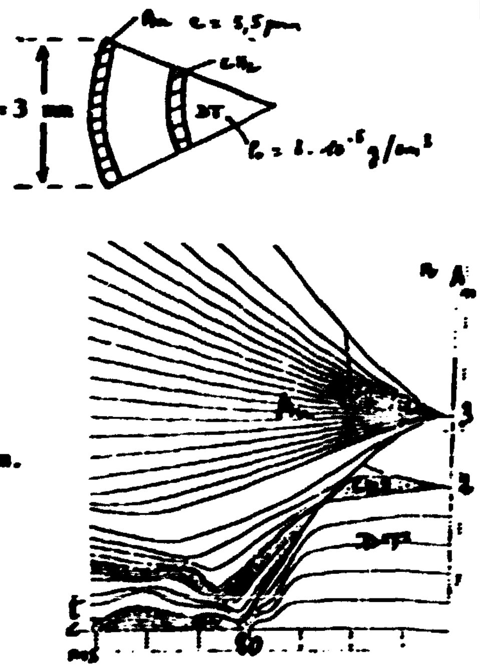

v_{max} pusher ∽ 4.10^6 cm/s

T_{max} DT ∽ 500 eV

$\int \rho\, dr$ ∽ 10^{-3}

Number of neutrons ∽ 10^6 to 5.10^6

But : hydrodynamic instability problem.

Fig.8 - Implosion diagram

.../...

4 - LIGHT ION-TARGET INTERACTION AT HIGH POWER DENSITIES

4-1 - Energy deposition evolution during the target heating

DEPION's evaluation

- high Z target : Au
- 4 MeV protons
- P ∼ 200 TW/cm^2

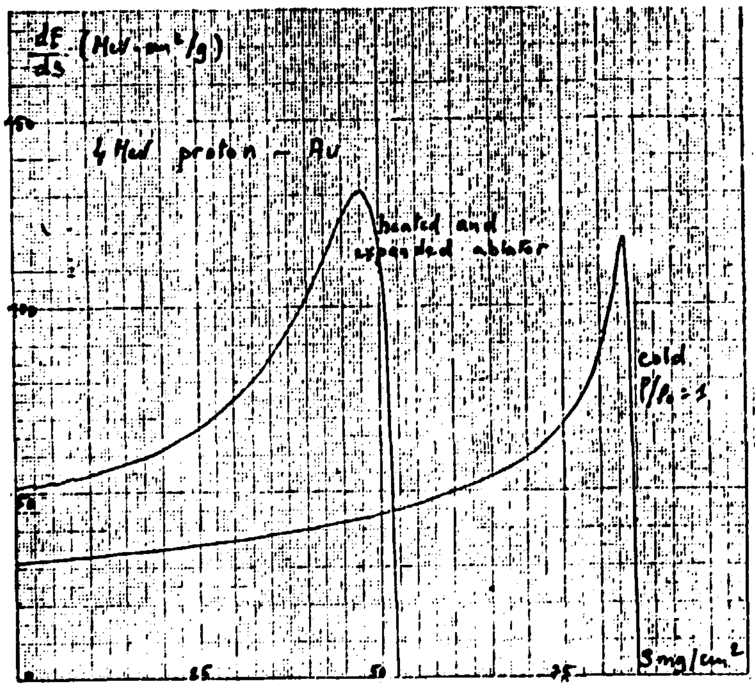

Fig. 9

The strong shortening of proton range in heated and expanded ablator implies a decrease of pellet performances; the results suggest that an accurate study of ablator structure must be made.

4-2 - Implosion performances evaluations

. Target

Ø pellet = 4 mm
gold ablator
Fe-Au pusher

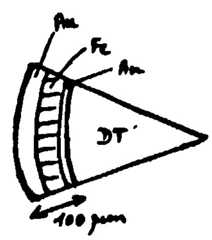

. Proton Beam

200 TW/cm^2 1 MJ Δt = 10 ns

. <u>Energy deposition</u>

Maximum temperature in ablator $\sim$ 230 eV.

. <u>Implosion characteristics</u>

$v_{max\ pusher} \sim 1{,}2.10^{7}$ cm/s

$T_{max\ DT} \sim 8 - 13$ keV

$\rho_{max\ DT} \sim 24$ g/cm^{3}

$\int \rho\, dr \sim 1{,}8.10^{-1}$

Gain $\sim$ 5

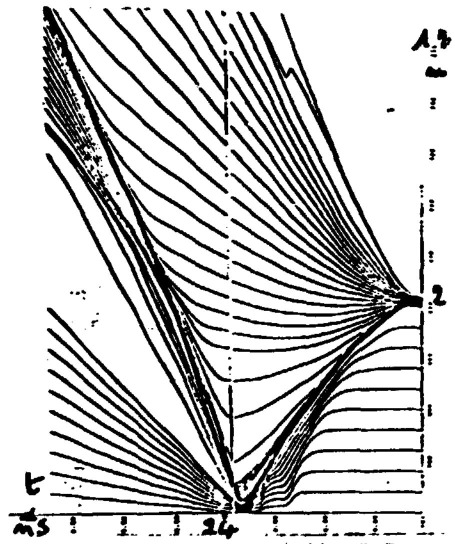

<u>Fig. 10</u> - Implosion diagram

This target is not optimized and better performances can be expected with a more adapted ablator structure.

CONCLUSIONS

DEPION model coupled to an hydrodynamic code provides an evaluatio of light ion energy deposition characteristics in composite heated and expanded targets.

At low power densities available on Sidonix (I $\sim$ 200 kA/cm^{2}?) the proton range shortening is already significative especially in low Z targets. Future hydrodynamic experiments on Sidonix will permit to suppo and verify these theoretical evaluations.- Implosion simulations in these conditions indicate the possibility to obtain thermonuclear neutrons evidence from I $>$ 200 kA/cm^{2}; however hydrodynamic instabilities could seriously degrade implosion performances in these high $r/\Delta r$ targets.

At high power densities required for pellet fusion, the strong ion range shortening is very important, as already shown by different authors as Mehlhorn, and implies an accurate ablator structure research.

.../...

REFERENCES

/1 / - CAMARCAT N. et al., PALAISEAU, July 81

/2 / - BRIOLAT R. et al., APS 81

/3 / - DUFOUR J.M., internal Report

/4 / - MEHLHORN T.A., Sand. 80-0038, May 80.